JOURNAL OF MATERIALS SCIENCE 24 (1989) 1095–1102

A study of various characteristics of supported NiO/bentonite catalyst used in the polymerization of methyl methacrylate

S. A. HASSAN, S. A. SELIM, M. A. MEKEWI, S. HANAFI
Department of Chemistry, Faculty of Science, Ain Shams University, Cairo, Egypt

Several samples of a supported NiO/bentonite catalyst were studied after pretreatment at either 300 or 500° C. The TGA results revealed that at 300° C, a fraction of nickel nitrite remains stabilized by the bentonite matrix. This fraction reaches its maximum level in samples IVa and Va (or 15 and 20% NiO w/w, respectively). From a study of the surface characteristics, it could be concluded that the nitrite fraction is located in the narrower pores of the catalyst system. The activity tested in the polymerization of MMA indicated that samples IVa and Va are the most active ones. The importance of the surface factor as well as the degree of fractional surface coverage by Ni^{2+} ions, or equivalently by the corresponding anions, could be tested. The results showed that the polymerization process proceeds via an anionic mechanism as enhanced by the presence of NO_2^- ions; the effect becoming much more pronounced in samples IVa and Va. The high stereospecific nature of the produced polymer in all cases can be attributed to the bentonite support effect, being activated by dispersing nickel oxide or other nickel species in its layer structure at both temperatures studied.

1. Introduction

Polymerization of some vinyl monomers by montmorillonite clays, and in particular bentonite has been studied previously [1, 2]. The catalyst activity was found to increase markedly by subjecting it to either thermal or chemical pretreatment. Activity due to thermal treatment was attributed to a modification in the characteristic pore system of the clay in addition to the action of Lewis acid sites created from the removal of adsorbed water [1]. It has been shown by Warshaw *et al.* [3] that heating the mineral to its dehydroxylation temperature (500–800° C) could not generally affect its whole structure. Acid treatment, on the other hand, was shown to lead to evolution of a somewhat different pore system and creation of Brønsted acid sites which were considered responsible for the observed activity [1, 4]. A destruction of the montmorillonite structure was claimed upon acid treatment with the retention of the aluminium silicate layer [5].

Polymerization of methyl methacrylate has been studied in several investigations in the absence of some inorganic compounds (see e.g., [6–8]). Nickel oxide, for instance, was found to catalyse the polymerization process ionically, whereas nickel nitrate having the highest catalytic activity produced polymers with the lowest molecular weight. Lead oxide, on the contrary, was found to polymerize methyl methacrylate by a radical mechanism that proved to be ineffective for styrene and acrylonitrile polymerization processes.

In the present study, nickel oxide was supported on bentonite at various concentration ratios through pretreatment either at 300° C or 500° C. Other factors affecting the support itself such as effective thermal or acid pretreatments were avoided. Such supported oxide systems were noticed to be of commercial importance for low-pressure coordination polymerization of olefins [9]. Studies on physicochemical characteristics of these systems and their influence on the mechanism of the polymerization process are still largely incomplete. Here, the catalyst composition, its thermal gravimetric profile as well as the surface characteristics were studied with special reference to their influence on the activity in the bulk polymerization of methyl methacrylate at 80° C.

2. Experimental details

2.1. Materials

2.1.1. Catalyst

The different samples of supported nickel oxide on bentonite were prepared by impregnating the preweighed amount of bentonite (Prolabo product) with the appropriate quantities of nickel nitrate solution. The mixture was stirred thoroughly to homogeneity and gradually dried at 110° C overnight. The dried product was then subjected to thermal treatment at either 300 or 500° C for a fixed time of 4 h, chosen on the basis of previously obtained results [1]. Samples treated at 300° C were designated as Ia, IIa, IIIa, IVa and Va corresponding to a NiO content of 2, 5, 10, 15 and 20% wt/wt, respectively. Another series treated at 500° C was designated as Ib, IIb, IIIb, IVb and Vb with the same NiO content.

2.1.2. Monomer

Stabilized methyl methacrylate was purified by shaking with 20% NaOH solution to remove the quinone

0022–2461/89 $03.00 + .12

inhibitor, followed by washing several times with bidistilled water then with ammonium acetate for neutrality. The product was dried over $CaCl_2$, vacuum distilled and stored at about 6° C over anhydrous sodium sulphate. The purity of the monomer was checked by measuring its refractive index.

2.2. Techniques

2.2.1. TGA

Thermogravimetric analysis of different catalyst samples was carried out in the presence of static air at a heating rate of 10° C min^{-1} using a Stanton–Redcroft thermobalance type 750/770 connected to a Kipp and Zonnen BD9 two-channel automatic recorder.

2.2.2. XRD

Some selected samples of bentonite support and supported NiO/bentonite catalyst were examined by using a Philips X-ray diffractometer, Model PW-1010.

2.2.3. BET-surface area and pore analysis

Adsorption–desorption isotherms of pure nitrogen on the surface of different catalyst samples were measured at 77 K using conventional volumetric apparatus. Specific surface areas and total pore volumes were calculated from the isotherms by applying the BET equation [10]. A value of 0.162 nm^2 was adopted for the molecular area of the adsorbed nitrogen.

2.2.4. Catalytic activity

The catalytic activity of various samples was measured in the bulk polymerization of methyl methacrylate. For this purpose, the freshly distilled monomer was introduced into the polymerization tube together with a weighed sample of the catalyst (2.5 % wt/wt of the monomer). The reaction tube was sealed under a dry flow of nitrogen gas and then placed in a thermostat adjusted at 80° C for 48 h. After cooling to room temperature, the tube was carefully opened and the contents were dissolved in acetone with occasional shaking. The solution was filtered to remove the catalyst and the polymer was precipitated by running the solution in a calculated amount of methanol (10 ml of alcohol for each 1 ml of the reaction mixture). The polymer produced was filtered, washed and dried under vacuum at 40° C till constant weight. Catalytic activity, [A], was expressed in terms of polymer yield (%), calculated as the (weight of the produced polymer/weight of the monomer used × 100).

2.2.5. Molecular weight from viscosity measurements

The specific and intrinsic viscosities of the polymer–acetone solutions were determined by applying Huggin's equation [11] in the form

$$\eta_{sp}/C = [\eta] + K[\eta]^2 C$$

where η_{sp}/C is known as the reduced viscosity which is a function of the molecular weight (η_{sp} is the specific viscosity for the given polymer concentration C expressed in grams per 100 ml of solution), $[\eta]$ is the intrinsic viscosity which is considered as a limiting value of the reduced viscosity, and K is Huggin's constant which is characteristic for the solvent used.

The specific viscosity, η_{sp}, was measured for different polymer concentrations using the suspended Ravikov viscometer [12] at a fixed temperature of 25° C. For the determination of intrinsic viscosity $[\eta]$, a plot of η_{sp}/C against C was constructed and the obtained straight line was extrapolated to zero concentration. Huggin's constant was calculated from the slope of this line. The average molecular weight, ($\bar{M}_w$), was then calculated according to Staudinger's equation modified by Kuhn [13]

$$[\eta] = K_m \bar{M}_w^a,$$

where K_m and a are constants related to the polymer–solvent system; taken as being 9.6 × 10^{-3} and 0.69, respectively for a polymethyl methacrylate–acetone system [14].

2.2.6. IR Study

A spectrophotometer model SP-200 G (UNICAM) was used for the IR-spectral study of the produced polymer.

3. Results and discussion

3.1. Thermal behaviour of bentonite, nickel salts and various supported nickel oxide samples

Figure 1 represents the TGA curves of pure bentonite and of various supported NiO samples preheated at 300° C. Three distinct steps can be observed in the temperature regions, 50–100° C, 280–380° C and 680–800° C. It is evident that the first step results from the evolution of physically adsorbed water coming mostly from pure bentonite (curve B). The dehydroxylation of the clay is observed in the temperature region,

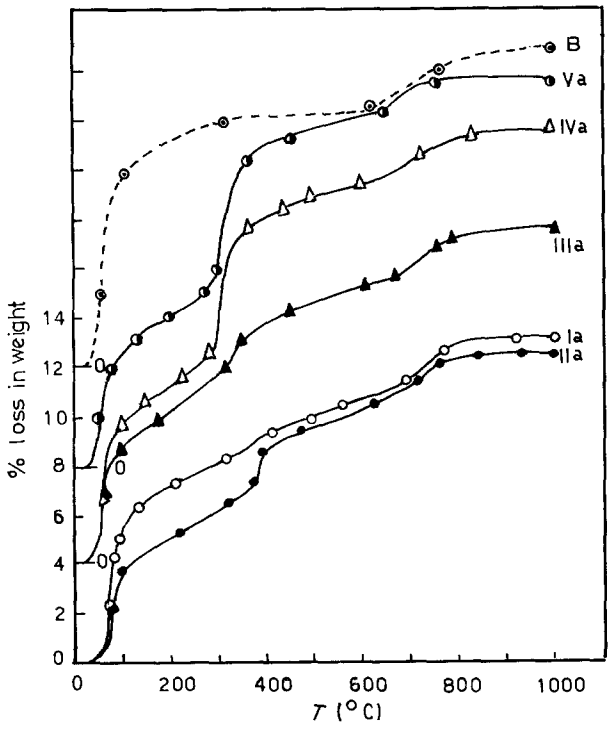

Figure 1 TGA curves (% loss in weight plotted against T(° C)) of pure bentonite support (B) and of various supported NiO/bentonite samples pretreated at 300° C.

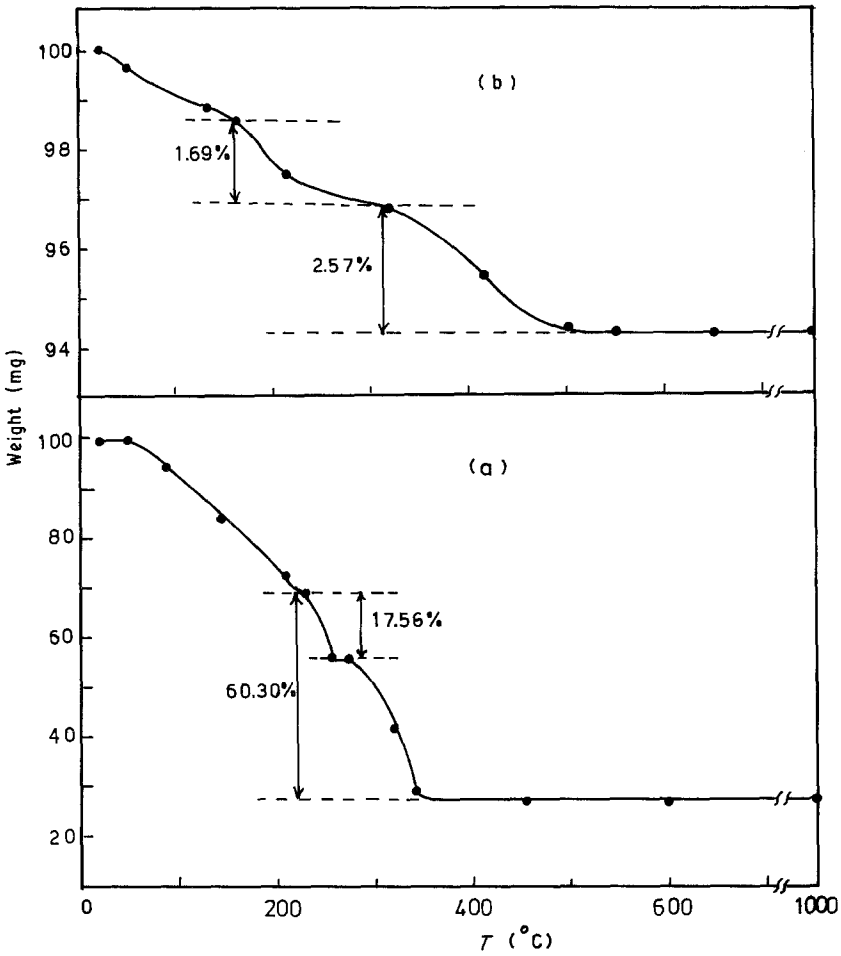

Figure 2 (a) TGA curve (weight, in mg, plotted against T(° C) of pure Ni $(NO_3)_2$ salt. (b) TGA curve of nickel oxide produced by heating $Ni(NO_3)_2$ for 4 h at 500° C.

680–800° C, which is reproduced by all catalyst samples studied. However, the loss in weight taking place in the region 280–380° C for the different supported samples cannot be assumed to arise from bentonite, as the latter does not exhibit such a distinct step. It seems, therefore, that this step can be attributed to the presence of undecomposed nickel salt. It is accompanied by a noticeable shift towards lower temperature as salt concentration increases. For more investigation, separate TGA was carried out for pure nickel nitrate, the curve of which is shown in Fig. 2a. It is clear that the first stage of the weight loss occurring below 220° C is due to the evolution of water of crystallization of the nitrate salt. The second stage represents the decomposition of the anhydrous salt as described elsewhere [15], which takes place in two steps, namely, at 225–270° C and at 270–350° C. By simple calculation from the weight losses, the first of these steps seems to be due to the evolution of oxygen to form the nitrite according to

$$Ni(NO_3)_2 \rightarrow Ni(NO_2)_2 + O_2$$

(theoretical loss = 17.51%). If we base our calculation on the anhydrous salt, the experimental loss was found to be 17.56%; being in good agreement with the theoretical value calculated for the nitrite formation. The second step indicates the decomposition of the nitrite to the respective oxide. The total loss according to the equation

$$Ni(NO_3)_2 \rightarrow NiO + \text{gaseous products},$$

is 59.11% as compared with the corresponding experimental loss of 60.30%. It is difficult, however, to conclude whether the nitrite form remains as such at 300° C or recombines with the evolved oxygen to reform the nitrate once more. The nitrite seems not to decompose immediately after the oxygen evolution but becomes stabilized, to some extent, by the clay matrix in the temperature range 255–275° C. This brings about the belief that all samples preheated at 300° C can be considered to contain some undecomposed nickel nitrite as indicated from the step occurring in the region 280–380° C. This behaviour is much more pronounced in samples IVa and Va (c.f., Fig. 1).

For catalyst samples treated at 500° C, the TGA curves indicate that the adsorbed water at $T < 150°$ C is much less than in the case of samples pretreated at 300° C. The second decomposition stage seems to be markedly affected by this high treatment temperature, i.e., the nickel nitrate is completely converted to the oxide form without appearance of the nitrite step as shown in Fig. 3.

A trial was also made to investigate the nature of the oxide formed. To this aim, $Ni(NO_3)_2$ was heated under the same conditions of the catalyst pretreatment, namely, 4 h at 500° C and stored in a dessicator. The TGA curve of the obtained oxide is illustrated in Fig. 2b, possessing three distinct steps, namely, in the temperature regions, < 130° C, 160–250° C and 300–350° C. The first step represents the loss of physically adsorbed water, whereas the two other steps arise most probably as a result of the loss of some oxygen from the oxide according to

$$Ni_{24}O_{28} \xrightarrow[(1.7\%)]{-O_2(1)} Ni_{24}O_{26} \xrightarrow[(2.51\%)]{-1\frac{1}{2}O_2(2)} Ni_{24}O_{23}$$

As indicated from Fig. 2b, step 1 is accompanied by a

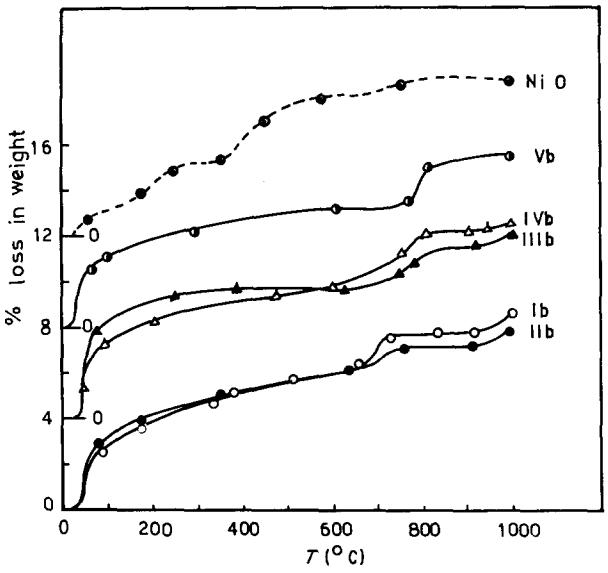

Figure 3 TGA curves (% loss in weight plotted against T(° C) of pure NiO and of various supported NiO/bentonite samples pretreated at 500° C.

weight loss of 1.69% which coincides with the theoretical value of 1.7%. Step 2 is accompanied by a 2.57% loss, being comparable with the corresponding calculated value of 2.51%. Such a reduction process was observed previously by some other oxides [16]. The obtained results lead us to believe that $Ni_{12}O_{11.5}$ when exposed to atmospheric air reverts back to the form $Ni_{12}O_{14}$ (or $NiO_{1.166}$).

3.2. X-ray investigation of the original bentonite and various supported samples

The data of the XRD analysis of the original bentonite support were published elsewhere [1]. The obtained spacings of hk reflections were those characteristic of the sodium form of bentonite (e.g., d = 1.190, 0.528, 0.445, 0.362, 0.256, 0.239, 0.209, 0.169, 0.161 and 0.149 nm). According to MacEwan [17], the results indicated bentonite with low substitutions of iron and magnesium for aluminium (namely, d = 0.169, 0.161 and 0.149 nm), assuming a typical formula [1] of

$$[Si_{7.76}Al_{0.24}]^{IV} \times [Al_{3.10}Fe^{3+}_{0.38}Fe^{2+}_{0.04}Mg_{0.52}]^{VI} \times O_{20}(OH)_4Na_{0.68}$$

The bentonite sample treated thermally at 300° C showed the same pattern exactly, whereas that treated at 500° C showed the anhydrous modification pattern (e.g., d = 0.970, 0.448 and 0.322 nm; with the disappearance of the aluminium oxide trihydrate peaks of d = 0.239 and 0.209 nm). In general, the whole bentonite structure remained almost unchanged under the applied thermal conditions. On the other hand, only for samples of NiO content $\geqslant$ 15% wt, peaks of d = 0.240 and 0.209 nm appeared again which seemed most probably to be characteristic of the supported NiO. This was evidenced by the increase noticed in their relative intensities by changing the temperature from 300° C to 500° C, yet no other phases could be detected.

3.3. Surface characteristics of the bentonite and various supported samples

Adsorption–desorption isotherms of nitrogen at −196° C for all samples preheated at 300° C and 500° C were of type II of Brunauer's classification [18]. Samples preheated at 300° C exhibited closed hysteresis loops except samples IIa and IIIa; the closure pressure being varied between 0.35 and 0.40 p/p_0. All samples preheated at 500° C exhibited closed hysteresis loops the closure pressure of which was shifted towards higher relative pressure, namely, 0.55–0.65 p/p_0.

The obtained data of specific surface area (S_{BET}), BET-C constant, total pore volume ($V_{p\,0.95}$) taken at 0.95 p/p_0, and average pore radius ($\bar{r}_h^{pp}$) assuming parallel plate model for which the superscript (pp) is used, are summarized in Table I. All these parameters were calculated from the adsorption–desorption isotherms.

By comparing the data obtained with those of pure bentonite, it is evident for sample Ia that an increase in area has occurred with a corresponding decrease in average pore radius, $\bar{r}_h^{pp}$, and a small decrease in the total pore volume, $V_{p_{0.95}}$. This evolution of area can be interpreted in view of the penetration of NiO between the bentonite sheets causing some expansion by which a new area from narrow pores is exposed. A corresponding increase in $V_{p_{0.95}}$ would have been expected but as the supported oxide covers part of the internal pore walls, a resultant small decrease is obtained instead.

TABLE I Surface characteristics for pure bentonite and various supported catalyst samples treated at 300° C and 500° C

Catalyst sample	S^*_{BET} ($m^2 g^{-1}$)	S_t ($m^2 g^{-1}$)	BET-C constant	$V_{p0.95}$ ($ml\,g^{-1}$)	$\bar{r}_h^{pp}$ (nm)
Bentonite	62.6	62.0	28	0.1087	1.75
Ia	81.1	80.0	7	0.1006	1.25
IIIa	55.5	58.5	10	0.0647	1.15
IIIa	58.2	58.8	9	0.0833	1.39
IVa	61.3	54.0	7	0.0811	1.30
Va	85.5	81.0	10	0.1108	1.30
Ib	73.8	73.5	8	0.1108	1.50
IIb	86.2	94.0	11	0.1268	1.45
IIIb	71.1	76.0	10	0.1034	1.45
IVb	74.5	72.0	7	0.0956	1.30
Vb	79.4	78.9	7	0.1092	1.40

* S_{BET} of pure NiO is 65.3 $m^2 g^{-1}$.

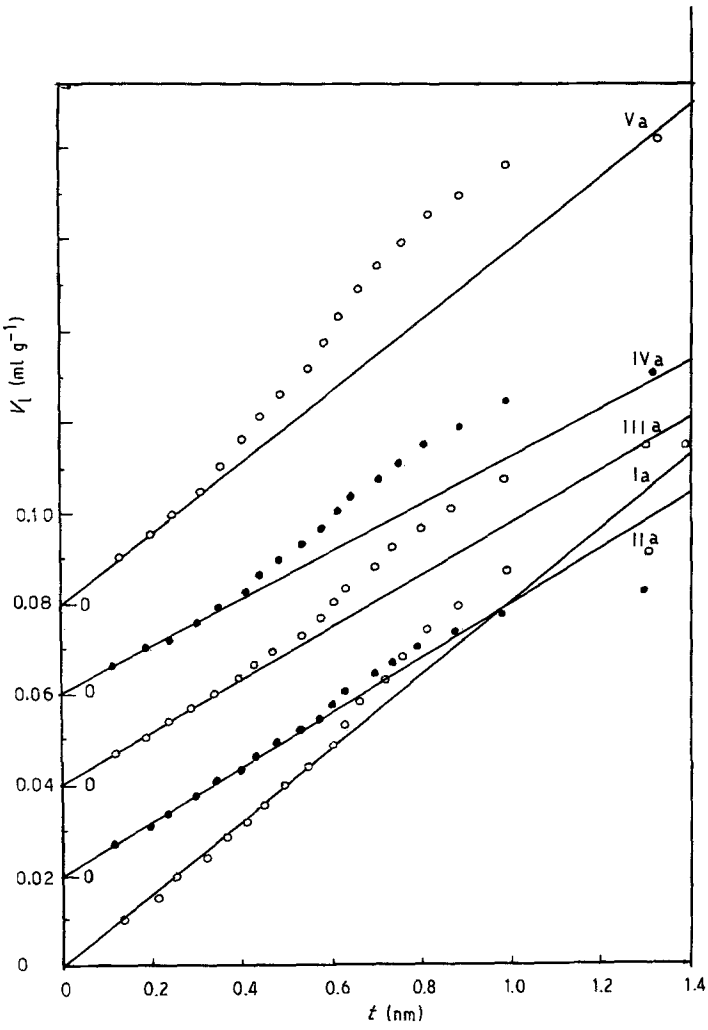

Figure 4 V_l–t plots for various samples of the supported NiO/bentonite catalyst preheated at 300° C.

Upon increasing the NiO content to 5%, sample IIa, more oxide seems to penetrate into the pores but still not deeply. This results in narrowing and/or blocking of some of the pores with small entrances which thereby may lead to a marked decrease in both S_{BET} and $V_{p_{0.95}}$. However, in the higher concentration region, up to 15% NiO (IIIa and IVa), a deeper penetration between bentonite sheets takes place and a gradual increase in both S_{BET} and $V_{p_{0.95}}$ is observed. As NiO increases to 20%, (Va), an enhanced expansion of the solid matrix occurs, which appears to result not only from the deeper penetration of the oxide but also from the escape of a great deal of evolved gaseous products resulting from the decomposition of the nitrate. Generally, the parallelism of the variation of both S_{BET} and $V_{p_{0.95}}$ with NiO content reflects, most probably, the layer structure of the bentonite support.

Pretreatment of the catalysts at 500° C seems to bring almost complete decomposition of the nitrate, as revealed from TGA, beside some sintering effect. Both these effects may lead to somewhat higher areas, pore volumes and average pore radii. By comparing the obtained results with those obtained at 300° C, it is clear that sample IIb shows an increase in surface parameters instead of the decrease observed for sample IIa. This may be understood in view of the different effects of the decomposition of the adsorbed nitrate especially of small concentration. This small concentration would not permit deep penetration of the formed oxide into the pore system of bentonite. If thermal decomposition of the original nitrate is incomplete, it would lead to some blocking of pores as in sample IIa, where a fraction of nitrate still exists as nitrite. We believe that due to an increased potential field inside the pores arising from the opposite walls, this fraction of undecomposed nitrite is probably situated in the narrower pores. In contrast, if the decomposition is complete, some expansion of pores would be expected from the evolution of gaseous products as in sample IIb.

For pore structure analysis, reference t-curves were constructed by several investigators based on adsorption of nitrogen on nonporous solids. For each catalyst sample, an appropriate t-curve was chosen on the basis of BET-C constants, which in each case should be of the same order in both the reference t-curve and the catalyst under investigation. In the present study, the t-curve of Mikhail *et al.* [19] based on non-porous solids with low BET-C constant was adopted for all samples studied.

From the adsorption data, V_l–t plots were constructed, where V_l is the volume of nitrogen in ml g^{-1} and t is the statistical thickness in nm. A straight line passing through the origin was obtained in each case. The slope of this line gave the specific surface area, S_t in m^2 g^{-1}. The agreement between S_{BET} and S_t was the main criterion for the correct choice of the t curve used in the analysis (Table I).

From the V_l–t plots shown in Figs 4 and 5, an upward deviation is observed for all catalyst samples

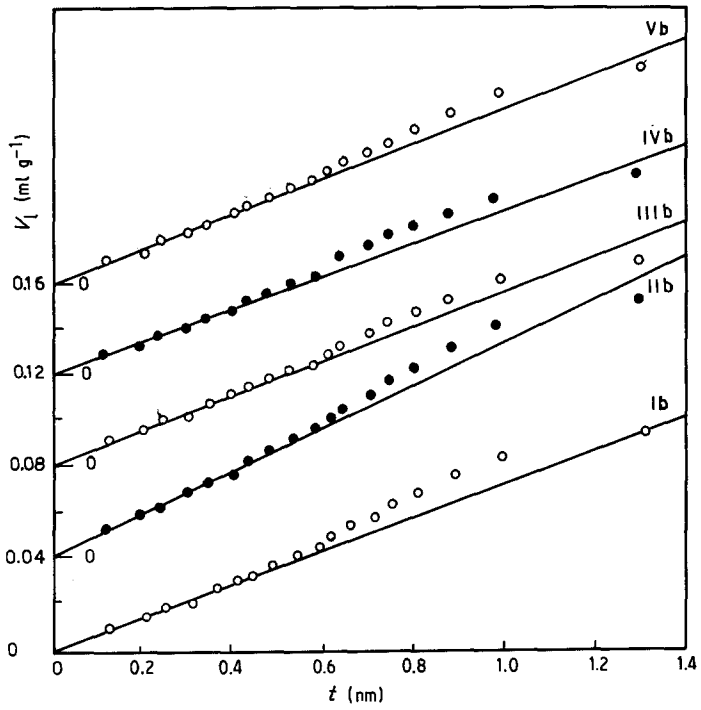

Figure 5 V_l–t plots for various samples of the NiO/bentonite catalyst preheated at 500° C.

pretreated at 300 and 500° C which reverts back at higher t-values showing the samples to be predominantly mesoporous.

For catalysts pretreated at 300° C, the marked narrowing and possibly blocking of some of the pores of sample IIa is reflected in its V_l–t plot where the slope of the upward deviation is much reduced. At NiO content greater than 10%, (samples IVa and Va), not only does the upward deviation increase with the increase in NiO content indicating a high mesoporosity, but also another group of pores seems to appear. The commencement of the upward deviation is shifted from a t-value of ~ 0.6 nm for samples with NiO ⩽ 5% to a t-value of ~ 0.3 nm for samples with higher NiO content. This shows clearly the expansion of the support layer structure with the increase in NiO content.

The slope of the upward deviation observed for catalyst samples preheated at 500° C is markedly smaller than that observed for the corresponding samples preheated at 300° C, which may reflect some sintering effect. The effect becomes much pronounced for the sample Vb, where the linear part of the V_l–t plot is extended to a t-value of ~ 0.75 nm, followed by a very small upward deviation.

TABLE II Catalytic activity of various supported NiO/bentonite samples in the polymerization of MMA and characteristic parameters of the produced polymer

Catalyst sample	Polymer yield (%) [A]	$[\eta]$	$\bar{M}_w$	$\bar{P}$
Without Catalyst	3.9	4.35	7063	71
Ia	45.6	17.35	55084	551
IIa	68.0	23.90	83545	835
IIIa	75.9	29.20	111683	1117
IVa	99.8	41.84	188160	1882
Va	100.0	41.86	188225	1882
NiO	21.3	31.60	125228	1252
Ib	29.3	20.35	66178	662
IIb	32.0	22.93	78676	787
IIIb	37.3	26.99	99644	996
IVb	38.0	29.30	112238	1122
Vb	39.2	30.79	120604	1206

3.4. Catalytic activity of the investigated samples

The results of the activity of various supported NiO/bentonite samples, measured in the polymerization of methyl methacrylate (MMA), are summarized in Table II, where the activity is expressed in terms of polymer yield (%). In all experiments, the catalyst–monomer ratio was 2.5% wt/wt.

It is clear that the catalyst samples treated at 300° C are much more active than those treated at 500° C. Maximum activity (100% yield) is almost achieved by samples IVa and Va. Pure bentonite was found to be completely inactive, even those samples treated thermally under the same conditions of the supported catalyst samples; the results were exactly the same as without catalyst, i.e., [A] = 3.9%. In both series of catalysts studied, the activity increases by increasing the NiO content. However, in all cases, the activity exceeds considerably that of pure bulk NiO which was previously shown to catalyse this reaction ionically. It may be concluded, therefore, that not only the presence of NiO, but also the mode of its dispersion on bentonite surface are responsible for the activity data obtained.

By considering the intrinsic viscosity data, $[\eta]$, the corresponding molecular weights calculated according to the above mentioned equation [12], and the degree of polymerization ($\bar{p}$), it can be noticed that these characteristic parameters increase with the increase in NiO content; running in harmony with the results of catalytic activity. Of special interest is the fact that the molecular weight ($\bar{M}_w$) of the produced polymer over almost all catalyst samples, except IVa and Va, is less valuable than that of the polymer produced in presence of NiO alone. Over samples IVa and Va, the molecular weight of the polymer produced

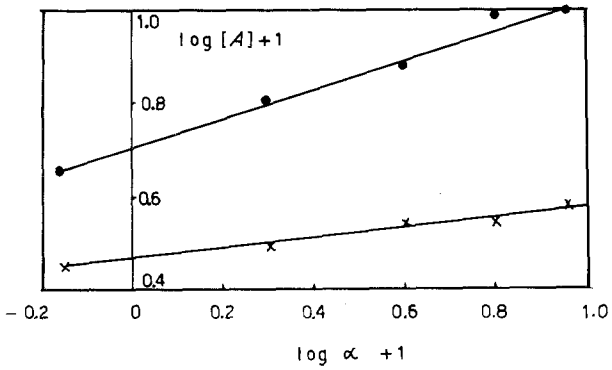

Figure 6 Log [*A*] (polymerization activity) (●), plotted against log α (fractional surface coverage of bentonite by nickel ions) (×).

is much higher which reflects their suitability as heterogeneous polymerization catalysts.

In an attempt to interpret the prevailing activity of samples IVa and Va, one should recall the results of surface characteristics and TGA. The importance of the surface factor in all cases can be evidenced from the constancy of specific activity parameter, $[A]/S_{BET}$, (average values = 0.012 for samples treated at 300° C and 0.005 for samples treated at 500° C). Moreover, the fractional surface coverage of bentonite by nickel ions, α_{Ni}^{2+}, was calculated according to the equation described elsewhere [20], taking the cross-sectional area of one Ni^{2+} ion, σ_{Ni}^{2+}, as $2.19 \times 10^{-20} m^2$. From the logarithmic relationship of the activity [*A*] as a function of α, illustrated in Fig. 6, it is clear that the activity in all cases depends strongly on the degree of surface coverage by nickel ions or equivalently by their anions; being considered as active centres. From results of TGA, it was shown that samples IVa and Va are characterized by the presence of a greater fraction of the undecomposed nitrite stabilized by bentonite matrix. It can consequently be supposed that the higher efficiencies of these two samples and the high molecular weights of the produced polymer may be attributed to the anionic coordination polymerization process enhanced by the presence of NO_2^- ions. A similar effect was recently observed but by NO^+ and NO_2^+ in some other polymerization processes [21].

3.5. IR investigation of the produced polymers

Typical IR spectra of isotactic and atactic structures, as well as those of polymethyl methacrylate obtained on pure bentonite and in presence of H_2SO_4 acid [22], are shown in Fig. 7. The IR spectra of polymethylmethacrylate formed on representative IVa and Va catalyst samples are also shown in this figure. The atactic structure is characterized by the presence of an absorption band at 9.45 μm, whereas in the isotactic structure, this band does not exist [23]. In the case of H_2SO_4 acid, the polymerization takes place via free radical mechanism, leading mainly to a polymer of atactic structure [24]. It is clear from our results, that the produced polymer has higher degree of isotacticity (IR spectra on IVa and Va samples). This stereospecific effect, observed unexceptionally for all studied catalyst samples, seems most likely to arise from the effect of bentonite support itself as shown from Fig. 7.

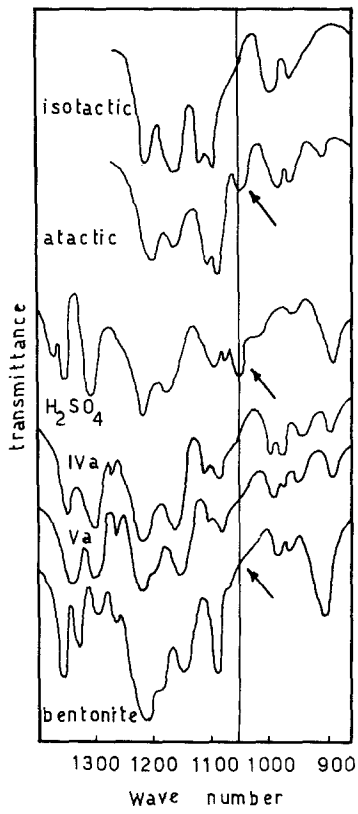

Figure 7 Infrared spectra of isotactic and atactic structures of PMMA and of polymethyl methacrylate produced on pure bentonite, in presence of H_2SO_4 acid and on the supported NiO/bentonite samples, namely, IVa (15% wt NiO) and Va (20% wt NiO).

4. Conclusion

From the obtained results, it can be concluded that the polymerization process, in the present study, follows most probably the anionic coordination mechanism enhanced by the presence of NO^- ions. The effect of these ions becomes much more pronounced in samples IVa and Va. The high isotacticity, i.e., the high stereospecific effect of all supported samples under study seems to arise from the bentonite support itself, being activated by dispersing nickel oxide or other nickel species in its layer structure at both 300 and 500° C.

References

1. S. A. HASSAN, A. M. MOUSA, M. M. ABDEL-KHALIK and A. A. ABDEL-AZIM, *J. Catal.* **53** (1978), 261.
2. K. I. SATAEV, E. A. ARIPOV and K. S. AKHMEDOV, "Adsorbtionye Svoistva Nekot." Fan-Publisher, Tashkent, USSR, (1970).
3. C. M. WARSHAW, P. E. ROSENBERG and R. ROY, *Clay Minerals Bull.* **4** (1960) 113.
4. P. N. ZELENZNYAK, V. D. KISLOV, N. N. KIRSANOV, G. A. DEMITRASH, B. F. GUSEV and S. N. BELYAEV; *Nefteprerab. Neftekhim. (Moscow)* **7** (1970) 13.
5. V. S. KOMAROV, L. I. POVOROZNYUK, N. I. PLYUSHEVSKII and YA. G. ZONOV; *Dokl. Akad. Nauk Beloruss, SSR* **9** (1965) 450.
6. A. B. MOUSTAFA, N. A. GHANEM and A. A. ABDEL-HAKIM; *J. Appl. Polym. Sci.* **20** (1976) 2643.
7. A. B. MOUSTAFA, M. A. ABDEL-GHAFFAR and A. S. BADRAN, *J. Polym. Sci, Polym. Chem. Edn,* **19** (1981) 719.
8. A. B. MOUSTAFA, A. M. RABIE and A. S. BADRAN, *Die Angew Makromol. Chem.* **103** (1982) 87.
9. A. CLARK, *Catalysis Rev.* **3** (1969) 145.

10. S. BRUNAUER, P. H. EMMETT and E. TELLER, *J. Amer. Chem. Soc.* **60** (1938) 309.
11. P. W. ALLEN, "Techniques of Polymer Characterization", Butterworths Scientific Publications, London (1959).
12. S. R. RAVIKOV, S. A. PAVLOVA and E. E. TVERDOCHLEBOVA, "Methods of Determination of Molecular Weights and Poly-dispersity of High Molecular Weight Compounds," Academic Press, Moscow (1963).
13. D. BRAUN, H. CHEDRON and W. KERN, "Techniques of Polymer Syntheses and Characterization", Wiley-Interscience (Translated), New York (1972) p. 67.
14. S. N. CHINAI, J. D. MATLACK, A. L. RESNICK and R. J. SAMUELS, *J. Polym. Sci.* **17** (1955) 391.
15. W. W. WENDLANDT; *Texas J. Sci.* **10** (1958).
16. S. A. SELIM, CH. A. PHILIP and R. SH. MIKHAIL, *Thermochimica Acta* **36** (1980) 287.
17. D. M. C. MacEWAN; "The Montmorillonite Minerals", Mineralogical Society of Great Britain Monographs, Chap 4, pp. 143–207.
18. S. BRUNAUER and P. H. EMMETT, *J. Amer. Chem. Soc.* **57** (1935) 1745.
19. R. SH. MIKHAIL, S. BRUNAUER and E. E. BODOR, *J. Colloid Interface Sci.* **26** (1968) 45.
20. YA. I. GERASIMOV, V. P. LEBEDEV and V. P. VENDILLO; "Practical Physical Chemistry", Part II, Kinetika i Kataliz, Moscow State University, Moscow (1963).
21. G. KOSSMEHL and J. HOCKER, Ger. Offen. DE 3, 224, 157 (Cl. C08G85/00), Dec. 1983; CA 100: 113337s.
22. N. A. MOUSA, MSc Thesis, Ain Shams University, Cairo, Egypt (1979).
23. R. ZBINDIN; "Infrared Spectroscopy of High Polymers.", Academic Press, New York (1964).
24. G. PISTOIA and M. A. VOSO, *J. Polym. Sci., Polym. Chem. Edn.* **14** (1976) 1811.

Received 30 April 1987
and accepted 28 April 1988